Progress In Electromagnetics Research Letters, Vol. 37, 133–142, 2013

GENERAL DECOUPLING NETWORK DESIGN BETWEEN TWO COUPLED ANTENNAS FOR MIMO APPLICATIONS

Mohamed A. Moharram* **and Ahmed A. Kishk**

Department of Electrical and Computer Engineering, Concordia University, Montreal, QC H3G 2W1, Canada

Abstract—A general design procedure of decoupling networks, between two coupled antennas, is proposed using a single transmission line connected between the input ports of the antennas at a specified distance. A rigorous analysis for the decoupling circuit is introduced considering the return loss of the antennas into calculations. Furthermore, using numerical optimization, enhancement of decoupling between the antenna ports achieved. Full-wave analysis and measurements are provided to verify the proposed technique.

1. INTRODUCTION

Recent wireless communication devices require multiple antennas to enhance the performance of the communication link by implementing multi-input-multi-output (MIMO) techniques. Mounting multiple small antennas, in proximity from each other, in these devices deteriorates the antenna efficiency, thus requires special handling for the coupling between antennas' ports to improve isolation, increase channel capacity [1], and subsequently bit rate [2].

1.1. Already Excising Decoupling Techniques

Reducing mutual coupling can be done naturally by having orthogonal polarization and patterns of antennas is proposed in [3, 4]. This technique requires placing antennas at specific places and orientations. However, the coupling level of these antennas increases as the distance between the elements decreases.

Away from having naturally decoupled antennas, a decoupling $\lambda/4$ or $3\lambda/4$ transmission line connected between matched, coupled two

Received 19 December 2012, Accepted 28 January 2013, Scheduled 31 January 2013

* Corresponding author: Mohamed A. Moharram (h_moh10@encs.concordia.ca).

antennas at specific distances from the antennas input ports, where the equivalent mutual impedance observed is pure imaginary, is a solution proposed in [5]. Additional matching sections are required for small antennas with fundamental mismatching [6] that increases the complexity and size of the antennas section as presented in [7]. Another analytical procedure in [8, 9] using factorization techniques to get the required scattering matrix of the decoupling network suggests using 180°-Hybrid to isolate two coupled antennas. Moreover, lumped elements implementation of the decoupling network for matched two antennas is presented in [10–12]. However, the design concerns of this technique are the physical dimensions of the elements, internal losses, and limited bandwidth.

Connecting neutralization lines between the radiating elements, in some antenna systems, reduces mutual coupling between antennas [13, 14]. This can be done by allowing a signal path from the radiating antenna to the other to eliminate the induced currents on the undesired one; resulting lower coupling level between antenna ports.

Inserting slits into the ground plane between the antennas can reduce the mutual coupling between antenna ports by suppressing surface waves between them [15–17]. Also, external decoupling structures are also presented through literature to eliminate near-field coupling between antennas. Meta-surfaces consisting of multiple layers of periodic metallic pattern are presented in [18, 19] forming an electromagnetic band-gap (EBG) structure suppressing the surface waves between the two antennas, thus reducing the mutual coupling between them. Other reactively loaded parasitic scatterers can be used to insure acceptable level of coupling between antennas ports [20].

1.2. Proposed Decoupling Technique

Here, a general design procedure for a decoupling network between two coupled antennas is introduced using a transmission line connected between the two ports at a specific distance from the antennas' ports. These antennas, in general, shouldn't be necessarily symmetric and perfectly matched. The return loss of the antennas are considered in the design procedure providing more possible solutions other than what is presented in [5]. Furthermore, having asymmetric antennas can be accounted for through the calculation with the advantage of having a degree of freedom to engineer resulting patterns for the two radiation modes of the antennas system. Afterwards, matching networks are then to be designed to match the resulting decoupled network to the $50\,\Omega$ impedance ports.

The decoupling network analysis and design are presented in Section 2. In Section 3, the simulated and measured results are

presented and finally we conclude at Section 4.

2. DECOUPLING NETWORK DESIGN PROCEDURE

A schematic of the proposed decoupling network is shown in Fig. 1. A decoupling transmission line of impedance Z_d and electrical length $\theta_d = \beta_d l_d$ is connected between the feeding ports of the antennas at specific electrical lengths θ_1 from the ports of the coupled antennas at t_a. Matching networks are then added following the decoupling network to match the input impedance of the two antennas system.

At t_a, the antennas measurements ports, the numerical evaluation of the 2-port S-parameters matrix can be expressed in terms of the return loss of port-1 α_1, return loss of port-2 α_2, and the insertion loss between ports 1 and 2, T_{12}.

The decoupling transmission line of arbitrary electrical length θ_d and characteristic impedance Z_d can be described by 4-port network S-parameters using even and odd modes analysis procedure explained in [21, 22]. The circuit can be completely described using only 4 S-parameters, namely: S_{11}, S_{21}, S_{31}, and S_{41}, due to symmetry and reciprocity of the circuit.

Connecting the 2-port network representing the antennas to the decoupling network through sections of electrical length θ_1 is shown in Fig. 1. The resulting transmission and reflection coefficients of the overall decoupling network can be written in the form

$$\begin{aligned} T &= S_{41} + \frac{S_{21}\left(XS_{31} - YS_{21}\right) + S_{31}\left(ZS_{21} - YS_{31}\right)}{XZ - Y^2}, \\ S_{11}^T &= S_{11} + \frac{S_{21}\left(XS_{21} - YS_{31}\right) + S_{31}\left(ZS_{31} - YS_{21}\right)}{XZ - Y^2}, \\ S_{22}^T &= S_{11} + \frac{S_{31}\left(XS_{31} - YS_{21}\right) + S_{21}\left(ZS_{21} - YS_{31}\right)}{XZ - Y^2}, \end{aligned} \tag{1}$$

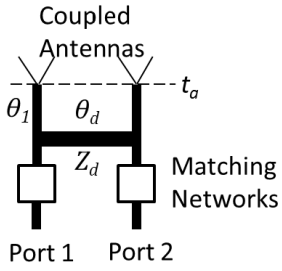

Figure 1. A schematic of the proposed decoupling circuit.

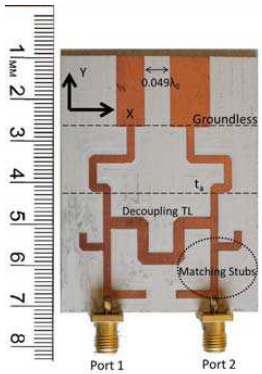

Figure 2. Decoupled closely mounted planner monopole antennas.

where the terms X, Y, and Z are defined as

$$X = \frac{\alpha_1 e^{-j2\theta_1}}{\alpha_1\alpha_2 e^{-j4\theta_1} - T_{12}^2 e^{-j4\theta_1}} - S_{11},$$
$$Y = \frac{-T_{12} e^{-j2\theta_1}}{\alpha_1\alpha_2 e^{-j4\theta_1} - T_{12}^2 e^{-j4\theta_1}} - S_{41}, \quad (2)$$
$$Z = \frac{\alpha_2 e^{-j2\theta_1}}{\alpha_1\alpha_2 e^{-j4\theta_1} - T_{12}^2 e^{-j4\theta_1}} - S_{11}.$$

The design goal is mainly to determine the values of θ_1, θ_d, and Z_d of the decoupling network to reach a specified decoupling criterion between the input ports. A simple manual optimization of the parameters of the mathematical model based can be invoked by choosing different characteristic impedances of the decoupling line and accordingly the electric length ranges from a simple plot of the above equations. A wide range of solutions can be obtained for decoupling networks featuring either deep decoupling situations, wide decoupling bandwidths, or in some cases acceptable decoupling situations with good matching within the operating bandwidth.

3. RESULTS AND DISCUSSIONS

The proposed technique is used to decouple a closely mounted ($0.049\lambda_0$, edge to edge, at 2.45 GHz) monopole antennas over a finite ground plane as shown in Fig. 2. This example is selected as a worst case scenario. The circuit is simulated using RO3006 microwave substrate with $\varepsilon_r = 6.15$ and thickness $h = 1.28$ mm.

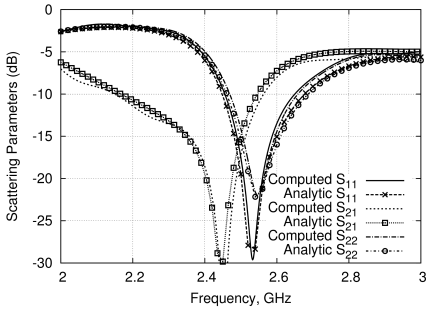

Figure 3. Comparison of the decoupling and matching levels after the decoupling network between analytical and full-wave numerical analysis (without using matching networks).

Having the simulated values of the insertion and transmission losses of the antennas at t_a at the design frequency with $\alpha_1 = 0.3676\angle -90.65°$, $\alpha_2 = 0.3857\angle -98.65°$, and $T_{12} = 0.51119\angle -15.8271°$, the proposed technique is used to design the decoupling circuit, which was found to be $\theta_1 = 41°$, $Z_d = 40\,\Omega$, θ_d has a range [217.2°, 327.2°] for a decoupling level larger that 15 dB; here $\theta_d = 232.6°$ for best decoupling with physical length extended to compensate for the effects of discontinuities (i.e., T-junctions) [21, 22]. A comparison of the obtained decoupling and matching levels just after the decoupling transmission line between analytical and full-wave analysis is shown in Fig. 3. Note that, other possible solutions can be obtained for different Z_d (i.e., solutions are not discrete).

The result of the proposed procedure, after using a double stub matching technique, is shown in Fig. 4 with a good matching with the full-wave simulation of the structure (small variations are due to imperfection in the fabrication process). A percentage bandwidth of 4% is obtained using this technique of both matching and decoupling which is better and simpler than what was presented in [7] for the same problem statement. The envelope correlation coefficient curve for the two antennas versus frequency is shown in Fig. 5 as defined in [23] comparing the values calculated from S-parameters (for lossless cases) and embedded far-fields of the antennas. It is clear that the previous two curves are very close to each other because the ohmic losses in the antennas are small [24].

Another implementation of the proposed technique is made for two PIFA antennas, each is designed to be matched when placed separately. The antenna system with decoupling network is shown in Fig. 6 with $0.057\lambda_0$ edge to edge separation at the design center

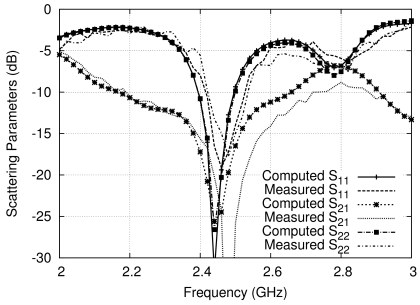

Figure 4. The Scattering parameters of the decoupling/matching circuit shown in Fig. 2 from measurements and full-wave analysis.

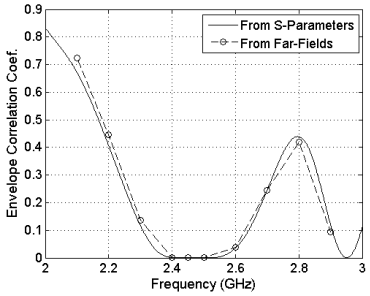

Figure 5. The envelope correlation coefficient of the decoupling/matching circuit shown in Fig. 2 calculated from S-parameters and embedded far-fields.

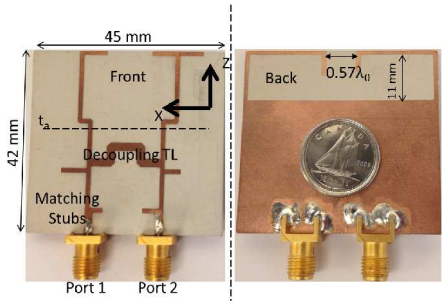

Figure 6. Another implementation of the proposed techniqe for 2 PIFA antennas each are matched when placed separately.

frequency 2.45 GHz. One way of miniaturization of the overall circuit is to design the antennas and decoupling transmission line for a high input impedance lines (60 Ω) which have small widths compared to the conventional 50 Ω lines. The final output ports are to be designed to give 50 Ω after the matching stage. The simulated antennas S-parameter values that are used to calculate the decoupling network parameters are $\alpha_1 = 0.42\angle -117°$, $\alpha_2 = 0.33\angle -105°$, and $T_{12} = 0.448\angle -155.9°$ with the 60 Ω reference impedance.

The resulting decoupling network parameters are chosen to maximize the available bandwidth for both decoupling and matching with values $Z_d = 50\,\Omega$, $\theta_1 = 41°$, and $\theta_d = 116°$. The simulated and

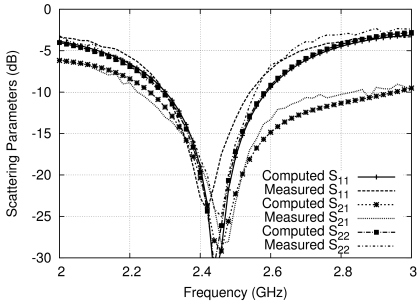

Figure 7. The measured and simulated S-parameters of the decoupling/matching circuit shown in Fig. 6.

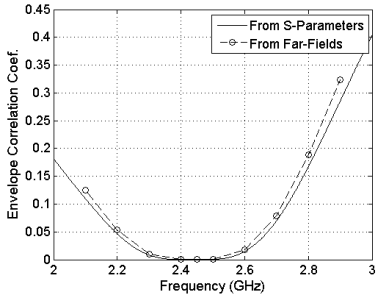

Figure 8. The envelope correlation coefficient of the decoupling/matching circuit shown in Fig. 6 calculated from S-parameters and embedded far-fields.

measured S-parameters of the proposed circuit is shown in Fig. 7 with good agreement. The achieved fractional bandwidth for this design is 12% (simulated) and 10% (measured). Also, the envelope correlation coefficient curve is shown in Fig. 8 with good agreement between the S-parameters and the embedded far-fields evaluations due to the small losses in the antennas.

It is worth mentioning that the first pair of antennas are already small with inherently mismatched ports when placed separately. Even by using matching networks, the maximum possible matching bandwidth is limited. This reflects the poor bandwidth achieved in the first example. On the other hand, the second pair of antennas are already designed to be matched with wide-band (minimum 24% at the same design frequency). The resulting bandwidth after decoupling and matching is better in this case (12%) than the previous one due to the antennas impedance variation nature.

4. CONCLUSION

The proposed technique provided a general decoupling network design procedure between two coupled asymmetric antennas taking into considerations non-perfectly matched ports conditions. The design procedure involved a rigorous analysis of the decoupling network with the ability to decouple asymmetric antennas if required. Several possible decoupling solutions were possible for either deep decoupling or large decoupling bandwidth. It was shown that the achieved

bandwidth depends mainly on the antennas; wide-band antennas (with almost constant impedance) can lead to a wide band decoupling bandwidth and vice-versa.

ACKNOWLEDGMENT

The authors would like to thank Rogers Corporation (http://www.rogerscorporation.com) for providing free laminate substrates.

REFERENCES

1. Foschini, G. and M. Gans, "On limits of wireless communications in a fading environment when using multiple antennas," *Wireless Pers. Commun.*, Vol. 6, No. 3, 331, 1998.
2. Paulraj, A., D. Gore, R. Nabar, and H. Bolcskei, "An overview of MIMO communications — A key to gigabit wireless," *Proceedings of the IEEE*, Vol. 92, No. 2, 198–218, Feb. 2004.
3. Getu, B. and J. Andersen, "The MIMO cube — A compact MIMO antenna," *IEEE Transactions on Wireless Communications*, Vol. 4, No. 3, 1136–1141, May 2005.
4. Zheng, J., X. Gao, Z. Zhang, and Z. Feng, "A compact eighteen-port antenna cube for MIMO systems," *IEEE Transactions on Antennas and Propagation*, Vol. 60, No. 2, 445–455, Feb. 2012.
5. Andersen, J. and H. Rasmussen, "Decoupling and descattering networks for antennas," *IEEE Transactions on Antennas and Propagation*, Vol. 24, No. 6, 841–846, Nov. 1976.
6. Best, S. R., "Small antennas," *Antenna Engineering Handbook,* 4th Edition, Chapter 6, 4–16, McGraw Hill, 2007.
7. Dossche, S., S. Blanch, and J. Romeu, "Optimum antenna matching to minimise signal correlation on a two-port antenna diversity system," *Electronics Letters*, Vol. 40, No. 19, 1164–1165, Sep. 2004.
8. Besoli, A., J. Romeu, L. Jofre, and F. De Flaviis, "Novel design methodology of matching networks based on the use of symmetry operators," *IEEE in Antennas and Propagation Society International Symposium, APSURSI' 09*, 1–4, Jun. 2009.
9. Zuo, S., Y.-Z. Yin, Y. Zhang, W.-J. Wu, and J.-J. Xie, "Eigenmode decoupling for MIMO loop-antenna based on 180 coupler," *Progress In Electromagnetics Research Letters*, Vol. 26, 11–20, 2011.
10. Chen, S.-C., Y.-S. Wang, and S.-J. Chung, "A decoupling tech-

nique for increasing the port isolation between two strongly coupled antennas," *IEEE Transactions on Antennas and Propagation*, Vol. 56, No. 12, 3650–3658, Dec. 2008.

11. Coaetzee, J. C., "Dual-frequency decoupling networks for compact antenna arrays," *International Journal of Microwave Science and Technology*, Vol. 2011, 2011.
12. Albannay, M. M., J. C. Coetzee, X. Tang, and K. Mouthaan, "Dual-frequency decoupling for two distinct antennas," *IEEE Antennas and Wireless Propagation Letters*, Vol. 11, 1315–1318, 2012.
13. Su, S.-W., C.-T. Lee, and F.-S. Chang, "Printed MIMO-antenna system using neutralization-line technique for wireless USB-dongle applications," *IEEE Transactions on Antennas and Propagation*, Vol. 60, No. 2, 456–463, Feb. 2012.
14. Diallo, A., C. Luxey, P. Le Thuc, R. Staraj, and G. Kossiavas, "Study and reduction of the mutual coupling between two mobile phone PIFAs operating in the DCS1800 and UMTS bands," *IEEE Transactions on Antennas and Propagation*, Vol. 54, No. 11, 3063–3074, Nov. 2006.
15. Chiu, C.-Y., C.-H. Cheng, R. Murch, and C. Rowell, "Reduction of mutual coupling between closely-packed antenna elements," *IEEE Transactions on Antennas and Propagation*, Vol. 55, No. 6, 1732–1738, Jun. 2007.
16. Li, J. F., Q. X. Chu, and X.-X. Guo, "Tri-band four-element MIMO antenna with high isolation," *Progress In Electromagnetics Research C*, Vol. 24, 235–249, 2011.
17. Zhang, S., B. K. Lau, Y. Tan, Z. Ying, and S. He, "Mutual coupling reduction of two PIFAs with a T-shape slot impedance transformer for MIMO mobile terminals," *IEEE Transactions on Antennas and Propagation*, Vol. 60, No. 3, 1521–1531, Mar. 2012.
18. Saenz, E., K. Guven, E. Ozbay, I. Ederra, and R. Gonzalo, "Decoupling of multifrequency dipole antenna arrays for microwave imaging applications," *International Journal of Antennas and Propagation*, Vol. 2010, 2010.
19. Bait-Suwailam, M., M. Boybay, and O. Ramahi, "Electromagnetic coupling reduction in high-profile monopole antennas using single-negative magnetic metamaterials for MIMO applications," *IEEE Transactions on Antennas and Propagation*, Vol. 58, No. 9, 2894–2902, Sep. 2010.
20. Lau, B. K. and J. Andersen, "Simple and efficient decoupling of compact arrays with parasitic scatterers," *IEEE Transactions on Antennas and Propagation*, Vol. 60, No. 2, 464–472, Feb. 2012.

21. Pozar, D. M., *Microwave Engineering,* 3rd Edition, 254, John Wiley & Sons, Inc., 2005.
22. Pozar, D. M., *Microwave Engineering,* 3rd Edition, 354–356, John Wiley & Sons, Inc., 2005.
23. Blanch, S., J. Romeu, and I. Corbella, "Exact representation of antenna system diversity performance from input parameter description," *Electronics Letters*, Vol. 39, No. 9, 705–707, May 2003.
24. Stein, S., "On cross coupling in multiple-beam antennas," *IRE Transactions on Antennas and Propagation*, Vol. 10, No. 5, 548–557, Sep. 1962.